Accepted Manuscript

Studies of defects and optical properties of $CaAl_{12}O_{19}:Ho^{3+}$ phosphor material

N. Singh, Vijay Singh, S. Watanabe, J.F.D. Chubaci, T.K.Gundu Rao, H. Gao, P. Mardina

PII: S0925-8388(15)31839-9

DOI: 10.1016/j.jallcom.2015.12.049

Reference: JALCOM 36138

To appear in: *Journal of Alloys and Compounds*

Received Date: 22 January 2015

Revised Date: 5 December 2015

Accepted Date: 8 December 2015

Please cite this article as: N. Singh, V. Singh, S. Watanabe, J.F.D. Chubaci, T.K.G. Rao, H. Gao, P. Mardina, Studies of defects and optical properties of $CaAl_{12}O_{19}:Ho^{3+}$ phosphor material, *Journal of Alloys and Compounds* (2016), doi: 10.1016/j.jallcom.2015.12.049.

Studies of defects and optical properties of $CaAl_{12}O_{19}:Ho^{3+}$ phosphor material

N. Singh [a], Vijay Singh [a,*], S. Watanabe [b], J.F.D. Chubaci [b], T. K. Gundu Rao [b], H. Gao [a], P. Mardina [a]

[a] Department of Chemical Engineering, Konkuk University, Seoul 143-701, Korea
[b] Institute of Physics, University of Sao Paulo, SP, 05508-090, Brazil

Abstract

Phosphor $CaAl_{12}O_{19}$ doped with holmium was synthesized by the low temperature solution combustion method. Powder X-ray diffraction (XRD) technique was used to find the phase formation and phase purity. The optical properties were studied using diffuse reflectance and photoluminescence (PL) spectroscopy. $CaAl_{12}O_{19}$:Ho exhibits three thermoluminescence (TL) peaks at approximately 140 ^{o}C, 260 ^{o}C and 440 ^{o}C. Electron Spin Resonance (ESR) studies were carried out to study the defect centers induced in the phosphor by gamma irradiation and also to identify the centers responsible for the TL process. Room temperature ESR spectrum of irradiated phosphor appears to be a superposition of at least four distinct centers. One of the centers (center I) with an isotropic g factor 2.0115 is tentatively assigned to an intrinsic O^- type center. This center relates with the TL peak at 140 ^{o}C. Center II with an axially symmetric g-tensor with principal values $g_{||}$=2.0283 and $g_{\perp}$=2.0058 is identified as an O_2^- ion and appears to correlate also with the 140 ^{o}C TL peak. Center III with an isotropic g-factor 2.0011 is assigned to an F^+ -type center (singly ionized oxygen vacancy) and is the likely recombination center for the two low temperature TL peaks. Another center with an isotropic g-value 2.0043 is visible after 300 ^{o}C thermal anneal and is also attributed to an F^+ center (center IV). This center appears to be associated with the high temperature TL peak at 440 ^{o}C.

Keywords: phosphor; defect centers; Ho^{3+} ions; photoluminescence, electron spin resonance

*Corresponding author:
E-mail: vijayjiin2006@yahoo.com (V. Singh)
Tel.:82-2-450-0536; Fax.: 82-2-458-3504

1. Introduction

Spectroscopic properties of rare-earth ions in inorganic host lattices have been investigated in recent years from the viewpoint of luminescence applications as well as basic research [1-3]. In this context, magnetoplumbite crystal structure provides different crystallographic sites for hosting rare-earth ions [4-6]. It is reported in the literature that $CaAl_{12}O_{19}$ crystallizes in a hexagonal magnetoplumbite structure with a 12-fold coordinated Ca^{2+} site. Further there are five independent Al^{3+} crystallographic sites; one tetrahedron, three octahedral and an unusual trigonal bipyramid with oxygen ions providing five-fold coordination [7-9].

It will be interesting to understand the type of defect centers that can be formed in this magnetoplumbite structure. From previous studies, it is clear that $CaAl_{12}O_{19}$ is a good host material with excellent luminescent properties when doped with a suitable activator. Even though several studies on rare-earth and transition metal ions doped $CaAl_{12}O_{19}$ are available [7-11], reports on holmium ion doped $CaAl_{12}O_{19}$ are very rare. Knowledge of the defect centers which can be formed in phosphor materials is useful while understanding luminescence mechanisms and in phosphor applications. The identification and classification of defect centers which are formed during irradiation are essential steps in understanding the mechanism of thermoluminescence (TL). Electron spin resonance (ESR) provides a convenient and sensitive technique for such a study. Over the past few decades, defect centers in phosphors were investigated using the ESR technique in order to study their correlations with TL glow peaks [12-17]. Authors have also carried out TL and ESR investigations on gamma-irradiated inorganic phosphors doped with rare-earth ions [15-19].

There is a wealth of information available in the literature on the luminescence properties of various holmium-doped systems [20-23]. To the best of our knowledge, there are no reports on the luminescence and defect center studies of holmium doped $CaAl_{12}O_{19}$ prepared by combustion synthesis. Combustion synthesis is a low temperature synthesis method that offers a unique synthesis route to produce complex oxides via a highly exothermic redox reaction between metal nitrates and an organic fuel. This present work reports the thermoluminescence, diffuse reflectance (DRF) and photoluminescence (PL) properties of Ho doped $CaAl_{12}O_{19}$ phosphor. Electron spin resonance (ESR) studies were also carried out to identify the defect centers responsible for TL peaks observed in $CaAl_{12}O_{19}$:Ho phosphor.

2. Materials preparation and analysis

The starting composition ratio of the calcium nitrate, aluminum nitrate and urea was based on the concepts of propellant chemistry. For the combustion, metal nitrates as oxidizers and urea as fuel were used. Holmium oxide (Ho_2O_3) was used as dopant. The concentration of holmium was 2 mol%.

Starting materials were crushed and ground in a ceramic dish with minimal quantity of de-ionized water to form solution. The dish was introduced into a muffle furnace preheated to 500±10 ^{o}C. The solution boiled, underwent dehydration, and finally decomposed with the evolution of large amount of gaseous by-products. The solution ignites and burns with a flame yielding voluminous solid mass. The entire combustion process was over in less than 5 min. The dish was immediately removed from the muffle furnace. The resultant foamy and

voluminous combustion ash mass was cooled and ground crushed into fine powder. The resulting fine powder was then further used for characterization.

The crystal phase of the prepared phosphors was analysed by an X-ray diffraction pattern measured using X'Pert PRO-MRD made in Netherlands. The UV-vis-NIR absorption of the samples was measured at room temperature by diffuse reflectance spectroscopy using a Cary 6000i UV-vis-NIR spectrometer equipped with an integrating sphere. Luminescence and luminescence excitation spectra were recorded using a Fluorolog 3-22 spectrometer (Jobin Yvon) with a 450W xenon lamp as an excitation source. TL measurements of irradiated samples have been carried out on a Thermo Scientific 4500 TL reader. A Bruker EMX ESR spectrometer operating at X-band frequency with 100 kHz modulation frequency was utilized for Electron Spin Resonance experiments. The g-factors of defect centers were calibrated using Diphenyl Picryl Hydrazyl (DPPH) as a standard sample. Temperature dependence of the ESR spectra was studied using a Bruker BVT 2000 variable temperature accessory. Calibrated ^{60}Co gamma chamber was used for irradiating the phosphor samples to gamma rays.

3. Results and discussion

3.1 X-ray diffraction

Fig. 1 shows the X-ray diffraction pattern of $CaAl_{12}O_{19}$:Ho phosphor. Sharp and intense X-ray diffraction peaks were observed due to the formation of high crystalline phosphor. The obtained peaks were well matched with the standard JCPDS card No. 07-0085. X-ray diffraction studies of as-formed product shows hexagonal phase even at a furnace temperature as low as 500 ^{o}C. No other impurity peaks are detected which indicate the presence of $CaAl_{12}O_{19}$ without any amorphous component. The hexagonal phase is not modified by the

addition of Ho in $CaAl_{12}O_{19}$ matrix. Hence the formed $CaAl_{12}O_{19}$:Ho is in pure hexagonal phase. Its formation is complete at the used furnace temperature without the need for further calcinations treatment.

3.2 Optical properties

3.2.1 Diffuse reflectance studies

The diffuse reflectance spectrum of Ho^{3+} doped $CaAl_{12}O_{19}$ powder phosphor in the 250-800 nm region is shown in Fig. 2. The spectrum consists of several absorption peaks which are at approximately 332, 343, 359, 383, 415, 450, 460, 467, 473, 481, 538, 548 and 646 nm. From Fig. 2 it is observed that the absorption bands $^5I_8 \rightarrow {}^3H_6$ (359 nm), $^5I_8 \rightarrow {}^5G_5$ (415 nm), $^5I_8 \rightarrow {}^5F_1$, $^5G_6$ (450/460 nm), $^5I_8 \rightarrow {}^5F_4$, $^5S_2$ (538/548 nm) and $^5I_8 \rightarrow {}^5F_5$ (646 nm) are relatively intense and sharp compared to other transitions. The bands corresponding to $^5I_8 \rightarrow {}^3F_4$ (332 nm), $^5I_8 \rightarrow {}^5G_3$ (343 nm), $^5I_8 \rightarrow {}^5G_4$ (383 nm), $^5I_8 \rightarrow {}^3K_8$ (467 nm), $^5I_8 \rightarrow {}^5F_2$ (473 nm), and $^5I_8 \rightarrow {}^5F_3$ (481 nm) are found to be very weak. In the present investigation, the $^5I_8 \rightarrow {}^5F_1$, $^5G_6$, transition has higher intensity when compared to other transitions. The assignments of the different absorption bands were made on the basis of energy level scheme of Ho^{3+} in $LaCl_3$ [24]. The assignments of the absorption bands originating from the ground level $^5I_8$ to various excited levels within the 4f shell are shown in Fig. 3a.

3.2.2 Photoluminescence studies

3.2.2.1 Excitation spectrum of $CaAl_{12}O_{19}$:Ho phosphor

In this section we focus on the photoluminescence properties of the $CaAl_{12}O_{19}$:Ho phosphor. To understand the excitation paths of Ho^{3+} ions, the photoluminescence excitation spectrum of $CaAl_{12}O_{19}$:Ho phosphor, with the emission monitored at 546 nm at room temperature, is shown

in Fig. 3b. Strong sharp excitation peaks are observed which correspond to the f-f transitions from the $^5I_8$ ground state to the excited states of Ho^{3+} [20-25]. The spectrum contains excitation bands which were observed approximately at 332, 343, 359, 383, 415, 450, 460, 467, 473 and 481 nm and correspond to the $^5I_8 \rightarrow {}^3F_4$, $^5I_8 \rightarrow {}^5G_3$, $^5I_8 \rightarrow {}^3H_6$, $^5I_8 \rightarrow {}^5G_4$, $^5I_8 \rightarrow {}^5G_5$, $^5I_8 \rightarrow {}^5F_1$, $^5I_8 \rightarrow {}^5G_6$, $^5I_8 \rightarrow {}^3K_8$, $^5I_8 \rightarrow {}^5F_2$, and $^5I_8 \rightarrow {}^5F_3$ transitions of trivalent holmium respectively. It is to be noted that among the various absorption transitions of the Ho^{3+} ion, the $^5I_8 \rightarrow {}^5F_1$, $^5G_6$, (450/460 nm) transition, is known as the hypersensitive transition [26]. In the present investigation, the $^5I_8 \rightarrow {}^5F_1$, $^5G_6$, transition has higher intensity when compared to other transitions. In the recorded range, the excitation spectrum is observed to be almost similar to the diffuse reflectance spectrum of the sample in terms of their peak positions. The only difference between the excitation and diffuse reflectance spectrum is observed below about 340 nm which is most probably due to the absorption caused by the host material. Among these excitation bands, the $^5I_8 \rightarrow {}^5F_1$, $^5G_6$, transition was used to investigate the visible photoluminescence characteristics of Ho^{3+} ions in $CaAl_{12}O_{19}$:Ho phosphor due to sharpness and highest intensity of this peak. Also, in both the cases, the $^5I_8 \rightarrow {}^5F_1$, $^5G_6$ transition has highest intensity. Further, it should be noted that the significant excitation bands (420-500nm) are located at approximately the emission wavelength of commercial blue-LEDs (450-470nm) which indicates that the prepared material can be investigated to act as a blue exciting phosphor [27]. The assignment on all the bands in excitation spectrum is shown in the Fig. 3a.

3.2.2.1 Emission spectrum of $CaAl_{12}O_{19}$:Ho phosphor

The photoluminescence (PL) spectrum excited by 450 nm blue light of $CaAl_{12}O_{19}$:Ho is given in Fig. 3(c). Upon excitation at 450 nm, the luminescence spectrum of sample is dominated by

four emission bands peaking at approximately 489 nm, 546 nm, 647 nm and 751 nm owing to intra f-f transitions of Ho^{3+} ions. It is observed that there are two more emission peaks adjacent to the peak at 546 nm. These side bands are the stark components of the peak corresponding to the $^5I_8 \leftarrow {}^5F_4$, $^5S_2$ transition of Ho^{3+} ions and are due to the crystal field of the host matrix. The spectrum contains emission bands at approximately 489, 546, 647 and 751 nm. These bands correspond to the $^5I_8 \leftarrow {}^5F_3$, $^5I_8 \leftarrow {}^5F_4$, $^5S_2$, $^5I_8 \leftarrow {}^5F_5$ and $^5I_8 \leftarrow {}^5I_4$ transitions of trivalent holmium respectively. The intensity of the peak due to the $^5I_8 \leftarrow {}^5F_4$, $^5S_2$ transition lying in the green region is much larger than that of the peak due to the $^5I_8 \leftarrow {}^5F_3$, $^5I_8 \leftarrow {}^5F_5$ and $^5I_8 \leftarrow {}^5I_4$ transitions lying in the blue, red and near-infrared (NIR) regions respectively. These emission bands mostly cover the tricolor areas, blue at 489 nm, green at 546 nm and red at 647 nm. The intensity of the emission peak at 546 nm corresponding to the $^5I_8 \leftarrow {}^5F_4$, $^5S_2$ transition is larger than the other peaks. In previous reports, Ho^{3+}-doped phosphors such as $Y_2O_3:Ho^{3+}$ [22], $Gd_3Ga_5O_{12}:Ho^{3+}$ [28] and $CaGa_2S_4:Ho^{3+}$ [29] mainly exhibit green light emission. Besides visible emission, very weak NIR emission was also observed at around 751 nm corresponding to the transition from the $^5I_4$ state to the $^5I_8$ state. This is in agreement with the previous observations [30]. To clearly illustrate the PL process, the simplified energy level diagram is given in Fig. 3a. Upon excitation at 450 nm, electrons can be excited to the $^5F_1$, $^5G_6$ level. The excited electrons can non-radiatively relax to the $^5F_3$ state and recombine to the lower level of $^5I_8$ which gives the blue emission. It appears that the excited electrons can non-radiatively relax to the $^5F_4$, $^5S_2$ states and recombine to the lower level of $^5I_8$ which gives the strong green emission. The weak red emission centered at 647 nm corresponds to the $^5I_8 \leftarrow {}^5F_5$ transition. In addition, the weak 751nm emission peak is due to the $^5I_8 \leftarrow {}^5I_4$ transition. The assignment on

all the bands in absorption, excitation and emission spectra is shown in the Fig. 3a. Based on the observed results, its seems that the $CaAl_{12}O_{19}$:Ho phosphor has potential for green luminescence devices. It is well established that the phosphor coating in devices is continuously subjected to ionizing radiations in order to convert to visible light output. The formation of defect centers can be expected. In the next section, we have studied the defect centers formed in $CaAl_{12}O_{19}$:Ho phosphor using the ESR technique.

3.3 TL and ESR studies

$CaAl_{12}O_{19}$:Ho exhibits three TL glow peaks at approximately 140 ^{o}C, 260 ^{o}C and 440 ^{o}C after gamma irradiation (dose: 50 Gy). The main glow peaks are at 140 ^{o}C and 260 ^{o}C whilst a smaller peak is seen at approximately 440 ^{o}C. The glow curve is shown in Fig. 4. The glow curves for the samples were obtained at a heating rate of 4 °C/s.

The ESR spectrum at room temperature of gamma irradiated (dose: 10 kGy) $CaAl_{12}O_{19}$:Ho is shown in Fig. 5. Thermal annealing and microwave power dependence experiments indicate that at least four defect centers contribute to the observed ESR spectrum. The ESR lines associated with these centers are labelled in Fig. 5. The line labelled as I is due to a center characterized by an isotropic g-value equal to 2.0115 and 11 gauss line width.

The hexagonal aluminate $CaAl_{12}O_{19}$ has a magnetoplumbite structure with space group $P6_3/mmc$ with lattice constants a = 5.587 Å and b = 21.8929 Å [31]. Calcium has a 12-fold coordination, while Al^{3+} ions are distributed over five different coordination sites, which include three distinct octahedral, one tetrahedral and an unusual trigonal bipyramid providing a fivefold coordination by oxygen ions. There are spinel blocks with Al^{3+} in both tetrahedral and octahedral sites which are bound with intermediate mirror layers containing large cations.

In $CaAl_{12}O_{19}$:Ho phosphor, Al site may be expected to have mixed occupancy with partial replacement by Ca ions. Such replacements arising from antisite cation exchange or the cation exchange disorder is a point defect in crystal lattices wherein cations exchange positions. The concentration and distribution of these defects in crystal lattices influence the optical properties, electrical conductivity, ionic diffusion and the resulting chemical properties. The presence of such defects has been predicted by theoretical calculations [32] and confirmed by x-ray diffraction [33], x-ray absorption fine structure [34] and direct observation by advanced electron microscopy [35]. An example of the effect of cation exchange disorder on the luminescence properties is provided by a recent study of Cr^{3+} doped AB_2O_4 spinel compounds [36]. The site of Ca^{2+} ion in $CaAl_{12}O_{19}$ has D_{3h} symmetry with 12-fold coordination and the ionic radius of calcium ion is 1.34 Å in this coordination [37]. Al^{3+} ion has 0.39 Å. 0.535 Å and 0.48 Å ionic radii in octahedral, tetrahedral and five-fold coordinated sites respectively. Since the ionic radius of Ho^{3+} ion is 1.12 Å in 10-fold coordinated site, it is expected that it would replace Ca^{2+} ion. It may be mentioned that Merkle et al. [38] have pointed out that rare-earth ions occupy Ca^{2+} sites in $CaAl_{12}O_{19}$ lattice. The replacement of divalent calcium ions by trivalent holmium leads to excess net positive charge and the charge balance could be achieved by formation of Calcium vacancies or extra O^{2-} ions at nearby interstitial positions. In $CaAl_{12}O_{19}$:Ho, a number of trapping sites for the electron and hole on irradiation may be created due to antisite formation mentioned above which results from the interchange of the ions in the octahedral, tetrahedral positions and trigonal bipyramid positions by divalent and trivalent ions. Moreover, irradiation may create a change in the defects charge state and

impurities charge state in the lattice [39]. Some of the luminescent and optical properties of the phosphor will be possibly affected by these defects.

Cation disorder and non-stoichiometry can lead to several lattice defects in an oxide system [40] like $CaAl_{12}O_{19}$:Ho and these defects may serve as trapping centers. First principle calculations have shown that oxygen vacancies would more easily form with cation disorder than in a perfect cation-ordered system [41]. Thus with cation disorder irradiation can form F^+ centers by trapping electrons at oxygen vacancies. On the other hand, O^- ions can be formed by hole trapping at aluminum or calcium vacancies [42]. It is well known that holes can be localized on oxygen ions and the basis for the localization is the trapping of a hole at a O_2^- ion to form an O^- ion. In this ion, the unpaired spin occupies an oxygen *p* orbital. A nearby cation vacancy can provide stability to the hole at the oxygen ion by way of electrostatic attraction. The observed ESR line of center I is slightly broad and indicate a possible delocalization of the unpaired electron and an interaction with nearby aluminum or an impurity nuclei. Hence center I is attributed to an O^- ion stabilized by a nearby cation vacancy (a positive hole localized on an O_2^- ion neighboring a Ca^{2+}/Al^{3+} ion vacancy). The positive g-shift in the principal g-value of center I is in accordance with the model of a hole trapped in a p_z orbital on an oxygen ion. The observed features of center I ESR line are similar to those observed by Ibarra et al. [43] in $MgAl_2O_4$. Ibarra et al. carried out optical absorption measurements and ESR studies on $MgAl_2O_4$ spinel. They observed the ESR spectrum with g = 2.011 after x-irradiation. After taking into consideration the optical absorption spectra, they concluded that the ESR spectra is related to hole trapping at cation vacancies i.e., to V-type centers formed by hole trapping at oxygen ions surrounding cation vacancies.

The stability of center I was measured using a pulsed-thermal annealing method. After heating the sample up to a given temperature, where it is maintained for 3 minutes, it is cooled rapidly down to room temperature for ESR measurements. The thermal annealing behaviour of center I is shown in Fig. 6(a). It is observed that the center becomes unstable around 50 °C and decays in the temperature range 50 °C-240 °C. This decay appears to relate to the TL peak at 140 °C.

Center II shown in Fig. 5 does not exhibit any hyperfine structure and is characterized by an axially symmetric *g*-tensor with principal values $g_{||}$ =2.0283 and $g_{\perp}$=2.0058. In general, the most likely centers to be formed on gamma irradiation in an oxide system like $CaAl_{12}O_{19}$ are the V-centers, F-centers and F^{+} -centers (an electron trapped at an anion vacancy) [40]. In a study on the binary oxide system Y_2O_3-CaO, Osada *et al.* [44] have observed oxygen ions. ESR studies have shown that the ion is characterized by an axial *g*-tensor with principal values $g_{||}$= 2.0400 and $g_{\perp}$=2.0030. The oxygen ion has been ascribed to the superoxide ion O_2^- and is generated by adsorption of molecular oxygen by the binary oxide system. O_2^- ions with considerable *g*-anisotropy have also been observed in a number of zeolites and metal oxides [45-47]. It is to be noted that the $g_{||}$ value for the O_2^- ion was found to be highly matrix dependent and ranged between 2.0150 and 2.0800 and is controlled by the magnitude of the crystal-field from the cations. Based on these results, center II with a relatively large anisotropy in *g*-values in the present system is tentatively assigned to an O_2^- ion. The thermal annealing behaviour of center II is shown in Fig. 6(b). It is observed that the center becomes unstable around 60 ^{o}C and decays in the broad temperature range 60 ^{o}C - 220 ^{o}C. Hence, O_2^- ion could also be associated with the 140 ^{o}C TL peak along with the O^- ion.

The ESR line labelled as III in Fig. 5 is due to a center characterized by an isotropic g-value equal to 2.0011 and 4 gauss linewidth. In general, irradiation of oxide systems often produces F^+ centers (an electron trapped at an anion vacancy) [40]. Such a center was first observed in neutron irradiated LiF and a single broad line was seen with a g-factor 2.0080 and 100 gauss linewidth [48]. X-ray and gamma irradiation has also produced similar centers in alkali halides and oxides. These centers are characterized by a small g-shift, which may be positive or negative and the ESR line can be narrow or broad depending on the host system.

An anionic vacancy can trap an electron due to irradiation and this forms the basis for the formation of F^+ centers. Hyperfine interaction with the nearest-neighbor (nn) cations contribute to the linewidth. Defect center II formed in the present system is characterized by a small g-shift and the linewidth is not large. On the basis of these observations and considerations of the characteristic features of the defect centers likely to be formed in a system such as $CaAl_{12}O_{19}$:Ho, center III is tentatively assigned to an F^+ center. The thermal annealing behaviour of center III is shown in Fig. 6(c). It is observed that the intensity of the ESR line associated with this center decreases in the temperature range from about 60 ^oC to 330 ^oC. The decay of center III appears to encompass the region of the two low temperature TL peaks and thus could be the recombination center associated with 140 ^oC and 260 ^oC TL peaks.

Fig. 5 shows the relatively strong center III ESR line along with an inner shoulder in the high field region of the spectrum. This shoulder line could not be observed properly in thermal annealing experiments due to overlap from center III line. However this line could be seen clearly after the decay of center III. The line labeled as center IV is characterized by a g-factor equal to 2.0043 and 7 gauss linewidth. The ESR spectra corresponding to this center after

thermal anneal at 300 ^{o}C, 320 ^{o}C and 500 ^{o}C are shown in Fig. 7. The center is also tentatively assigned to an F^{+} center based on the reasons mentioned above. The thermal annealing behavior of center IV is shown in Fig. 8. There is scatter in the measured intensity due to poor signal strength of center IV. However the scattered decay points to the possibility of association of this center with the high temperature 440 ^{o}C TL peak.

Certain inferences have been made in this study on the role of observed defect centers in $CaAl_{12}O_{19}$:Ho and their correlations with the TL peaks. These inferences are based on pulse annealing experiments in ESR. Additional support to these inferences is provided by thermal annealing the irradiated phosphor in the TL instrument simulating the conditions of the TL experiment. The irradiated samples were warmed to 200 ^{o}C at a heating rate of 4 ^{o}C/sec in the TL instrument. The ESR spectrum recorded after cooling the sample to room temperature is shown in Fig. 7. Pulse annealing experiments in ESR indicate that (Fig. 6) center I (O^{-} ion) and center II (O_2^{-} ion) have almost decayed and center III (F^{+} center) ESR signal is reduced in intensity allowing center IV signal to be visible in the ESR spectrum after annealing at 200 ^{o}C. It is gratifying to note that the observed spectrum shown in Fig. 9 is in accordance with these expectations.

Alkaline earth aluminates have been found to be attractive hosts in luminescent studies due to their intricate structures. These structures are capable of generating more defect related traps when doped with rare-earths and transition metal ions. With the presence of non-equivalent sites, $CaAl_{12}O_{19}$ is particularly interesting as a host in these studies. ESR has been used along with luminescent investigations on $CaAl_{12}O_{19}$ and most of these studies are concerned with luminescence arising from dopant rare-earth and transition metal ions [9, 49,

50]. In europium doped $CaAl_{12}O_{19}$ [51], however, defects created due to ionizing radiation have been studied in connection with the observed TL along with the study of luminescent properties. In that study [51], a dominant TL peak at 240 ^{o}C is reported along with an unresolved shoulder peak at 174 ^{o}C. Irradiation has been found to create three defect centers and two of these centers are attributed to F^{+} centers. The F^{+} centers were found to have different thermal stabilities as in the present case of $CaAl_{12}O_{19}$:Ho phosphor. The TL glow peak temperatures in the present case are close to the ones observed in $CaAl_{12}O_{19}$:Eu. The high temperature peak (440 ^{o}C), however, is not reported in $CaAl_{12}O_{19}$:Eu phosphor most likely due to the limitations in the temperature range of the TL instrument. Apart from F^{+} centers, other centers like O^{-} and O_2^{-} ions are not reported.

With a view to observe the defect centers which may be formed in the absence of rare-earth ions in the alkaline earth lattice, pure $CaAl_{12}O_{19}$ has been irradiated with gamma rays and the observed spectrum recorded under similar conditions as irradiated $CaAl_{12}O_{19}:Ho^{3+}$ phosphor is shown in Fig. 10(a). Two distinct centers could be identified and these are labelled as center I and II in Fig. 10(a). Center I is characterized by a g-value equal to 2.0015 and has a linewidth of 3 gauss. On the other hand, center II has a g-value 2.0023 and a linewidth of 16 gauss. These two centers are tentatively assigned to F^{+} centers and correspond to center III and center IV observed in $CaAl_{12}O_{19}:Ho^{3+}$ phosphor, respectively. O^{-} and O_2^{-} ions are forming in very low concentrations as compared to the rare-earth ion doped phosphor and are barely seen in the spectrum shown in Fig. 10(a). These lines are indicated by a red rectangular block in Fig. 10(a). Fig 10(b) shows the ESR spectrum in pure $CaAl_{12}O_{19}$ system recorded with higher power (20 mW) and higher modulation amplitude (2 gauss). The ESR lines corresponding to O^{-}

and O_2^- ions are somewhat better seen and again are indicated by a rectangular block. It was mentioned earlier that the presence of Ho^{3+} ions at Ca^{2+} sites would lead to formation of negatively charged centers/ions in the phosphor lattice. It is gratifying to note that the observed relatively efficient formation of O^- and O_2^- ions in the doped phosphor is in accordance with this expectation.

4. Conclusions

Based on the results and discussions presented above, the following conclusions may be highlighted.

1) The $CaAl_{12}O_{19}$:Ho powders were synthesized directly through a simple propellant combustion method using low cost and non-toxic inorganic compounds as main precursors. Hexagonal phase without other crystalline phases was observed from XRD result.

2) The absorption bands could be assigned easily due to the transitions of the ground-level $^5I_8$ to higher energy levels. The positions and relative intensities of absorption peaks agree well with the excitation spectrum. Excitation spectrum was mostly located around 420-500 nm, consistent with the emission wavelength of the blue LED chip, which suggests a potential blue exciting phosphor.

3) The luminescence spectra recorded at an excitation wavelength 450 nm exhibited emission bands at around 489, 546, 647 and 751 nm correspond to the transitions $^5I_8 \leftarrow {}^5F_3$, $^5I_8 \leftarrow {}^5F_4$, $^5S_2$, $^5I_8 \leftarrow {}^5F_5$ and $^5I_8 \leftarrow {}^5I_4$ respectively. The transition $^5I_8 \leftarrow {}^5F_4$, $^5S_2$ observed in the green region is found to be more intense. Based on the photoluminescence results, synthesized

phosphor may play an important role in making the green producing phosphor for display applications and light emitting diodes.

4) $CaAl_{12}O_{19}$:Ho phosphor exhibits three TL peaks at 140 ^{o}C, 260 ^{o}C and 440 ^{o}C for a heating rate of 4 ^{o}C/s. Four defect centers have been identified in the irradiated phosphor based on ESR studies. These centers are tentatively assigned to an O^- ion, O_2^- ion and F^+ centers. O^- ion and the superoxide ion O_2^- correlate with the main 140 ^{o}C TL peak. One of the F^+ centers appears to be related to the two low temperature TL peaks and most likely acts as a recombination centers. The second F^+ center is associated with the high temperature TL peak at 440 ^{o}C.

Acknowledgements

This paper was supported by the KU Research Professor Program of Konkuk University. T. K. Gundu Rao is grateful to CAPES, Brazil for the research fellowship.

References

1. Fengwen Kang, Yihua Hu, Li Chen, Xiaojuan Wang, Haoyi Wu, Influence of Zn^{2+} and Si^{4+} codoping on luminescence properties of $CaWO_4$:Eu^{3+} phosphor, Materials Science and Engineering B, 178 (2013) 477-482
2. Fengwen Kang, YihuaHu, Li Chen, Xiao-uanWang, Haoyi Wu, Zhongfei Mu, Luminescent properties of Eu^{3+} in MWO_4 (M=Ca,Sr,Ba) matrix, Journal of Luminescence 135(2013)113-119
3. Si Chen, Yuhua Wang, Jia Zhang, Lei Zhao, Qian Wang, Lili Han, Luminescent properties of novel $K_3R(PO_4)_2$:Tb^{3+} (R=Y and Gd) phosphors for displays and lightings, Journal of Luminescence 150 (2014) 46-49.
4. Xin Min, Minghao Fang, Zhaohui Huang, Yan'gai Liu, Chao Tang, Tingting Qian, Xiaowen Wu, Synthesis and luminescence properties of nitrided lanthanum magnesium hexaluminate $LaMgAl_{11}O_{19}$ phosphors, Ceramics International, 40 (2014) 4535-4539.
5. Yuji Masubuchi, Tomoyuki Hata, Teruki Motohashi, Shinichi Kikkawa, Crystal structure of Eu-doped magnetoplumbite-type lanthanum aluminum oxynitride with emission site splitting, Journal of Solid State Chemistry, 184 (2011) 2533-2537.
6. Zhongyi Zhang, Yunhong Zhang, Xiaoli Li, Jianhua Xu, Yan Huang, VUV-UV luminescence of magnetoplumbite: $(Sr_{0.96}$-x$Ba_{0.04})Al_{12}$-y$MgyO_{19}$:Tbx, Journal of Luminescence, 128 (2008) 476-480.
7. Zhwan Dilshad Ibrahim Sktani, Ahmad Zahirani Ahmad Azhar, Mani Maran Ratnam, Zainal Arifin Ahmad, The influence of in-situ formation of hibonite on the properties of zirconia toughened alumina (ZTA) composites, Ceramics International, 40 (2014) 6211-6217.
8. M.G. Brik, Y.X. Pan, G.K. Liu, Spectroscopic and crystal field analysis of absorption and photoluminescence properties of red phosphor $CaAl_{12}O_{19}$:Mn^{4+} modified by MgO, Journal of Alloys and Compounds, 509 (2011)1452-1456.
9. Vijay Singh, R.P.S. Chakradhar, J.L. Rao, Dong-Kuk Kim, Photoluminescence and EPR studies of Cr-doped hibonite ($CaAl_{12}O_{19}$) phosphors, Solid State Sciences, 10 (2008) 1525-1532.
10. Wei Shu, Lingling Jiang, Siguo Xiao, Xiaoliang Yang, J.W. Ding, GeO_2 dopant induced enhancement of red emission in $CaAl_{12}O_{19}$:Mn^{4+} phosphor, Materials Science and Engineering: B, 177 (2012) 274-277.
11. Z.G. Nie, J.H. Zhang, X. Zhang, S.Z. Lü, X.G. Ren, G.B. Zhang, X.J. Wang, Photon cascade luminescence in $CaAl_{12}O_{19}$:Pr, Cr, Journal of Solid State Chemistry, 180 (2007) 2933-2941.
12. Sanjeev Menon, Bhushan Dhabekar, E. Alagu Raja, S.P. More, T.K. Gundu Rao, R.K. Kher, TSL, OSL and ESR studies in $ZnAl_2O_4$:Tb phosphor, Journal of Luminescence, 128 (2008) 1673-1678.
13. T.K. Gundu Rao, B.C. Bhatt, P.S. Page, Defect centers and thermoluminescence in Al_2O_3:Si,Ti, Radiation Measurements, 43 (2008) 295-299.
14. S. Watanabe, T.K. Gundu Rao, P.S. Page, B.C. Bhatt, TL, OSL and ESR studies on beryllium oxide, Journal of Luminescence, 130 (2010) 2146-2152.
15. Vijay Singh, T.K. Gundu Rao, Studies of defects in combustion synthesized europium-

doped $LiAl_5O_8$ red phosphor, Journal of Solid State Chemistry, 181 (2008) 1387-1392.
16. Vijay Singh, S. Watanabe, T.K. Gundu Rao, Ho-Young Kwak, Luminescence and defect centres in Tb^{3+} doped $LaMgAl_{11}O_{19}$ phosphors, Solid State Sciences, 12 (2010) 1981-1987.
17. Vijay Singh, S. Watanabe, T.K. Gundu Rao, J.F.D Chubaci, Ho-Young Kwak, Luminescence and defect centres in $MgSrAl_{10}O_{17}:Sm^{3+}$ phosphor, Journal of Non-Crystalline Solids, 356 (2010) 1185-1190.
18. Vijay Singh, S. Watanabe, T.K. Gundu Rao, J.F.D. Chubaci, Ho-Young Kwak, Characterization, photoluminescence, thermally stimulated luminescence and electron spin resonance studies of Eu^{3+} doped $LaAlO_3$ phosphor, Solid State Sciences, 13 (2011) 66-71.
19. Vijay Singh, S. Watanabe, T.K. Gundu Rao, Katharina Al-Shamery, Markus Haase, Young-Dahl Jho, Synthesis, characterisation, luminescence and defect centres in solution combustion synthesised $CaZrO_3:Tb^{3+}$ phosphor, Journal of Luminescence, 132 (2012) 2036-2042.
20. Junfeng Zhao, Xi Chen, Chunying Rong, Liping Yu, Shixun Lian, A tunable yellow emission from three-band emission of singly doped single-phased phosphor $BaY_2S_4:Ho^{3+}$, Journal of Rare Earths, 29 (2011) 436-439.
21. T. Wei, Q.J. Zhou, C.Z. Zhao, Y.B. Lin, Y.L. Zou, Y. Li, L.S. Zhang, Strong green light emission in Ho doped $Bi_4Ti_3O_{12}$ ferroelectric ceramics, Ceramics International, 39 (2013) 7211-7215.
22. Vijay Singh, Vineet Kumar Rai, Benjamin Voss, Markus Haase, R.P.S. Chakradhar, D. Thirupathi Naidu, Sang Hwan Kim, Photoluminescence study of nanocrystalline $Y_2O_3:Ho^{3+}$ phosphor, Spectrochimica Acta Part A: Molecular and Biomolecular Spectroscopy, 109 (2013) 206-212.
23. Wei Xie, Yinhai Wang, Changwei Zou, Jun Quan, Lexi Shao, A red-emitting long-afterglow phosphor of Eu^{3+}, Ho^{3+} co-doped Y_2O_3, Journal of Alloys and Compounds, 619 (2015) 244-247.
24. H. M. Crosswhite, Hannah Crosswhite, Norman Edelstein, Katheryn Rajnak, Parametric energy level analysis of $Ho^{3+}:LaC1_3$, The Journal of Chemical Physics, 67 (1977) 3002-3010.
25. V.R. Bandi, B.K. Grandhe, M.J ayasimhadri, K.J ang, H.S. Lee, S.S. Yi, J.H. Jeong, Photoluminescence and structural properties of $Ca_3Y(VO_4)_3$ RE^{3+} (=Sm^{3+}, Ho^{3+} and Tm^{3+}) powder phosphors for tri-colors, Journal of Crystal Growth 326 (2011) 120-123.
26. R.D. Peacock, Structure and Bonding, Berlin 22 (1975) 83-122.
27. S. Nakamura,G.Fasol, The Blue Laser Diode:GaN Based Light Emitters and Lasers, Springer, Berlin,1997.
28. J.C. Boyer, F. Vetrone, J.A. Capobianco, A. Speghini, M. Bettinelli, Yb^{3+} ion as a sensitizer for the upconversion luminescence in nanocrystalline $Gd_3Ga_5O_{12}:Ho^{3+}$, Chemical Physics Letters, 390 (2004) 403-407.
29. Chongfeng Guo, Chunxiang Zhang, Yühua Lü, Qiang Tang, Qiang Su, Luminescent properties of Eu^{2+} and Ho^{3+} co-doped $CaGa_2S_4$ phosphor, Physica status solidi (a), 201, (2004) 1588-1593.
30. T. Wei, Z. Chang, Q. J. Zhou, D. M. An, Z. P. Li, F. C. Sun, Bright green emission in

Ho doped $Bi_{1/2}Na_{1/2}TiO_3$ ferroelectric ceramics, Materials Letters, 115 (2014) 129-131.
31. A. Utsunomiya, K. Tanaka, H. Morikawa, F. Marumo, H. Kojima, Structure refinement of $CaO{\cdot}6Al_2O_3$, Journal of Solid State Chemistry, 75 (1988) 197-200.
32. M.M. Kuklja, Defects in yttrium aluminium perovskite and garnet crystals: atomistic study, Journal of Physics: Condensed Matter 12 (2000) 2953-2967.
33. A.P. Patel, M.R. Levy, R.W. Grimes, R.M. Gaume, R.S. Frigelson, K.J. McClellan, C.R. Stanek, Mechanisms of nonstoichiometry in $Y_3Al_5O_{12}$, Applied Physics Letters, 93 (2008) 191902.
34. J. Dong, K. Lu, Noncubic symmetry in garnet structures studied using extended x-ray-absorption fine-structure spectra, Physical Review B, 43 (1991) 8808.
35. D. Truong, M.K. Devaraju, T. Tomai, I. Honma, Direct Observation of Antisite Defects in $LiCoPO_4$ Cathode Materials by Annular Dark- and Bright-Field Electron Microscopy, ACS Applied Materials Interfaces, 5 (2013) 9926-9932.
36. N. Basavaraju, K.R. Priolkar, D. Gourier, S.K. Sharma, A. Bessiere, B. Viana, The importance of inversion disorder in the visible light induced persistent luminescence in Cr^{3+} doped AB_2O_4 (A = Zn or Mg and B = Ga or Al), Physical Chemistry Chemical Physics, 17 (2015) 1790-1799.
37. R.D. Shannon, Revised Effective Ionic Radii and Systematic Studies of Interatomic Distances in Halides and Chalcogenides, Acta Crystallographica Section A Acta Cryst. A32 (1976) 751-767.
38. L.D. Merkle, B. Zandi, R. Moncorge, Y. Guyot, H.R. Verdun, B. McIntosh, Spectroscopy and laser operation of Pr, Mg:$SrAl_{12}O_{19}$, Journal of Applied Physics, 79 (1996) 1849.
39. G. P. Summers, G. S. White, K. H. Lee, J. H. Crawford, Radiation damage in $MgAl_2O_4$, Physical Review B, 21 (1980) 2578-2584
40. V. Singh, V. Kumar Rai, S. Watanabe, T.K. Gundu Rao, L. Badie, I. Ladoux-Rak, Y.D. Jho, Synthesis, characterization, optical absorption, luminescence and defect centres in Er^{3+} and Yb^{3+} co-doped $MgAl_2O_4$ phosphors, Applied Physics B, 108 (2012) 437-446.
41. N. Yuan, X. Liu, F. Meng, D. Zhou, J. Meng, First-principles study of La_2CoMnO_6: a promising cathode material for intermediate-temperature solid oxide fuel cells due to intrinsic Co-Mn cation disorder, Ionics, 21 (2015) 1675-1681.
42. M.S. Holston, J.W. McClory, N.C. Giles, L.E. Halliburton, Radiation-induced defects in $LiAlO_2$ crystals: Holes trapped by lithium vacancies and their role in thermoluminescence, Journal of Luminescence, 160 (2015) 43-49
43. A. Ibarra, F.J. Lopez, Jimenez de Castro, V centers in $MgAl_2O_4$ spinels Physical Review B 44 (1991) 7256-7262.
44. Y. Osada, S. Koike, T. Fukushima, S. Ogasawara, T. Shikada, T. Ikariya, Oxidative coupling of methane over Y_2O_3-CaO catalysts, Applied Catalysis, 59 (1990) 59-74.
45. D.D. Eley, M.A. Zammitt, Spin centers and catalysis on γ-alumina, Journal of Catalysis, 21 (1971) 366-376.
46. K.M. Wong, J.H. Lunsford, Electron paramagnetic resonance study of Y-type zeolites. III. O2- on AlHY, ScY, and LaY zeolites, The Journal of Physical Chemistry, 74 (1971) 1165-1168.

47. J.H. Lunsford, ESR of adsorbed oxygen species, Catalysis Reviews 8 (1973) 135-157.
48. C.A. Hutchison, Paramagnetic resonance absorption in crystals colored by irradiation, Physical Review, 75 (1949) 1769-1770.
49. Y.I. Li, Y.Y. Ma, S. Ye, G.P. Hu, Q.Y. Zhang, Site-related near-infrared luminescence in $MAl_{12}O_{19}$ (M = Ca, Sr, Ba):Fe^{3+} phosphors, Materials Research Bulletin, 51 (2014) 1-5.
50. V. Singh, S. Borkotoky, A. Murali, J.L. Rao, T.K. Gundu Rao, S.J. Dhoble, Electron paramagnetic resonance and photoluminescence investigation on ultraviolet-emitting gadolinium-ion-doped $CaAl_{12}O_{19}$ phosphors, Spectrochimica Acta Part A: Molecular and Biomolecular Spectroscopy, 139 (2015) 1-6.
51. V. Singh, T. K. Gundu Rao, J-J. Zhu, Synthesis, photoluminescence, thermoluminescence and electron spin resonance investigations of $CaAl_{12}O_{19}$:Eu phosphor, Journal of Luminescence 126 (2007) 1-6.

Figure Captions

Fig. 1. Powder XRD pattern of $CaAl_{12}O_{19}:Ho^{3+}$ phosphor prepared at 500 ^{o}C along with the standard JCPDS pattern

Fig. 2. Diffuse reflectance spectrum of $CaAl_{12}O_{19}:Ho^{3+}$ phosphor

Fig. 3. (a) The transitions of the peaks are shown in energy level diagram of Ho^{3+} ion, (b) excitation spectrum of $CaAl_{12}O_{19}:Ho^{3+}$ phosphor (λ_{em}= 546 nm), and (c) Emission spectrum of $CaAl_{12}O_{19}:Ho^{3+}$ phosphor (λ_{ex}= 450 nm).

Fig. 4. TL glow curve of $CaAl_{12}O_{19}$:Ho at 4 ^{o}C/s for 50 Gy dose showing TL peaks at 140 ^{o}C, 260 ^{o}C and 440 °C respectively.

Fig. 5. Room temperature ESR spectrum of irradiated $CaAl_{12}O_{19}$:Ho phosphor (gamma dose : 10 kGy). Line labelled as I is due to an O^- ion. Center II line is assigned to an O_2^- ion and center III is attributed to a F^+ center.

Fig. 6. Thermal annealing behaviour of (a) center I, (b) center II and (c) center III in $CaAl_{12}O_{19}$:Ho phosphor.

Fig. 7. Room temperature ESR spectrum of irradiated $CaAl_{12}O_{19}$:Ho phosphor after thermal anneal at (a) 300 ^{o}C, (b) 320 ^{o}C and (c) 500 ^{o}C showing center IV ESR line.

Fig. 8. Thermal annealing behaviour of center IV in $CaAl_{12}O_{19}$:Ho phosphor.

Fig. 9. Room temperature ESR spectrum of irradiated $CaAl_{12}O_{19}$:Ho phosphor (gamma dose: 10 kGy) after warming to 200 ^{o}C at a heating rate of 4 ^{o}C/S in the TL instrument.

Fig. 10. (a) Room temperature ESR spectrum of irradiated pure $CaAl_{12}O_{19}$ (microwave power: 10 mW and 1 gauss modulation). (b) Spectrum recorded with higher microwave power and modulation (microwave power: 20 mW and 2 gauss modulation). The rectangular boxes show the lines arising from low intensity O^- and O_2^- ions.

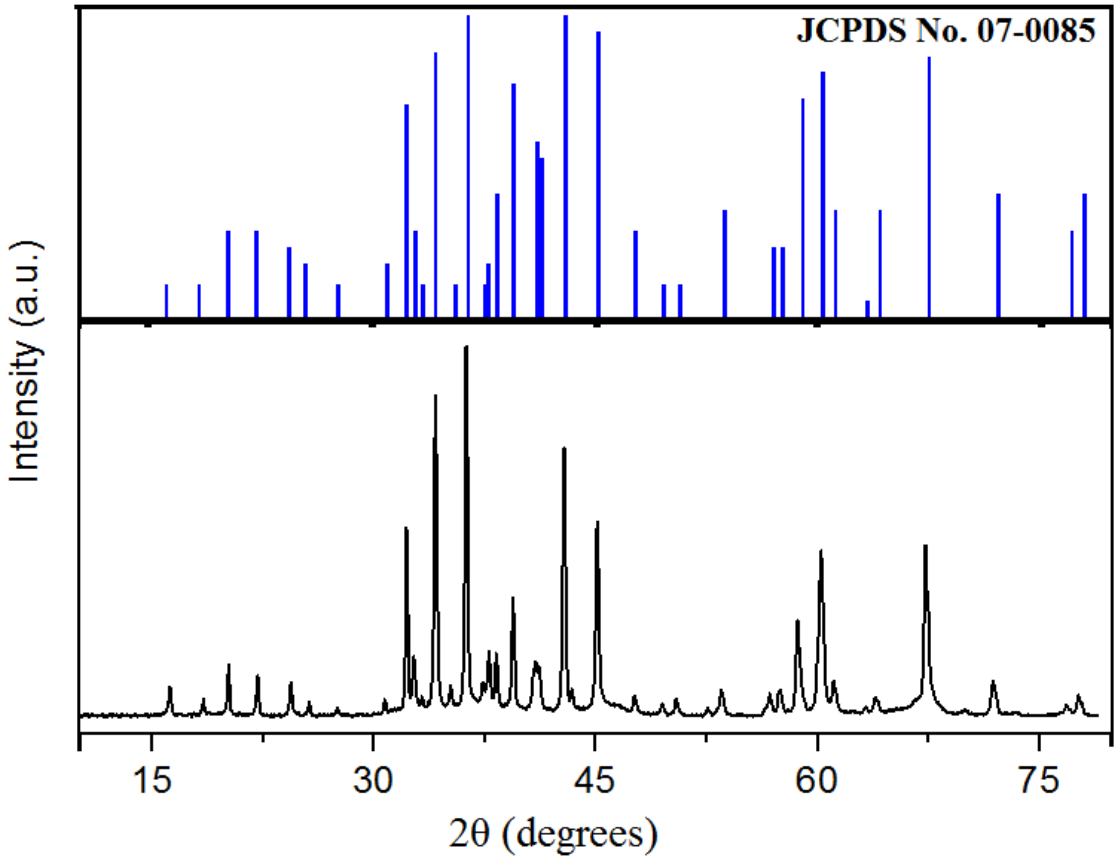

Fig. 1. Powder XRD pattern of $CaAl_{12}O_{19}:Ho^{3+}$ phosphor prepared at 500 ^{o}C along with the standard JCPDS pattern

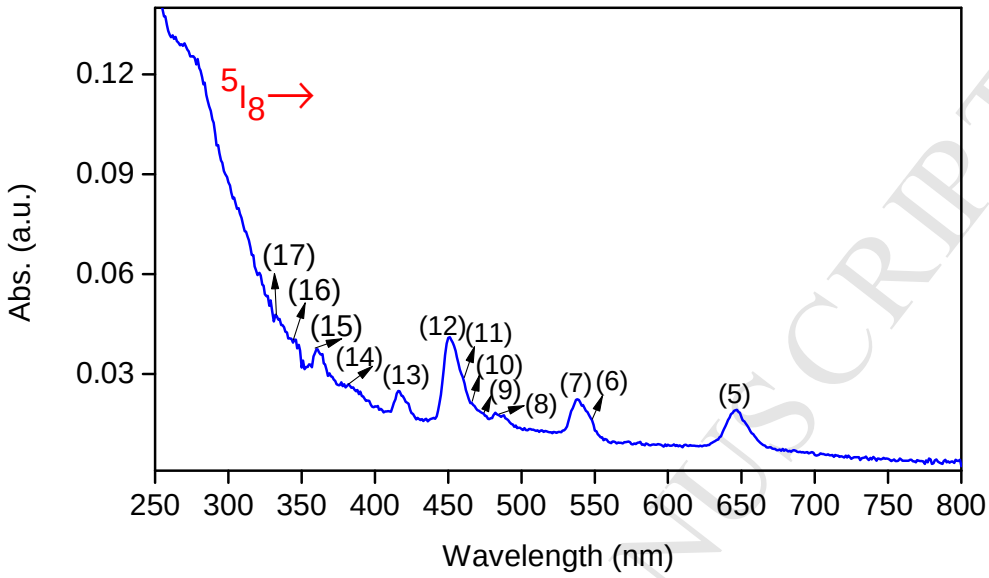

Fig. 2. Diffuse reflectance spectrum of $CaAl_{12}O_{19}:Ho^{3+}$ phosphor

(a)

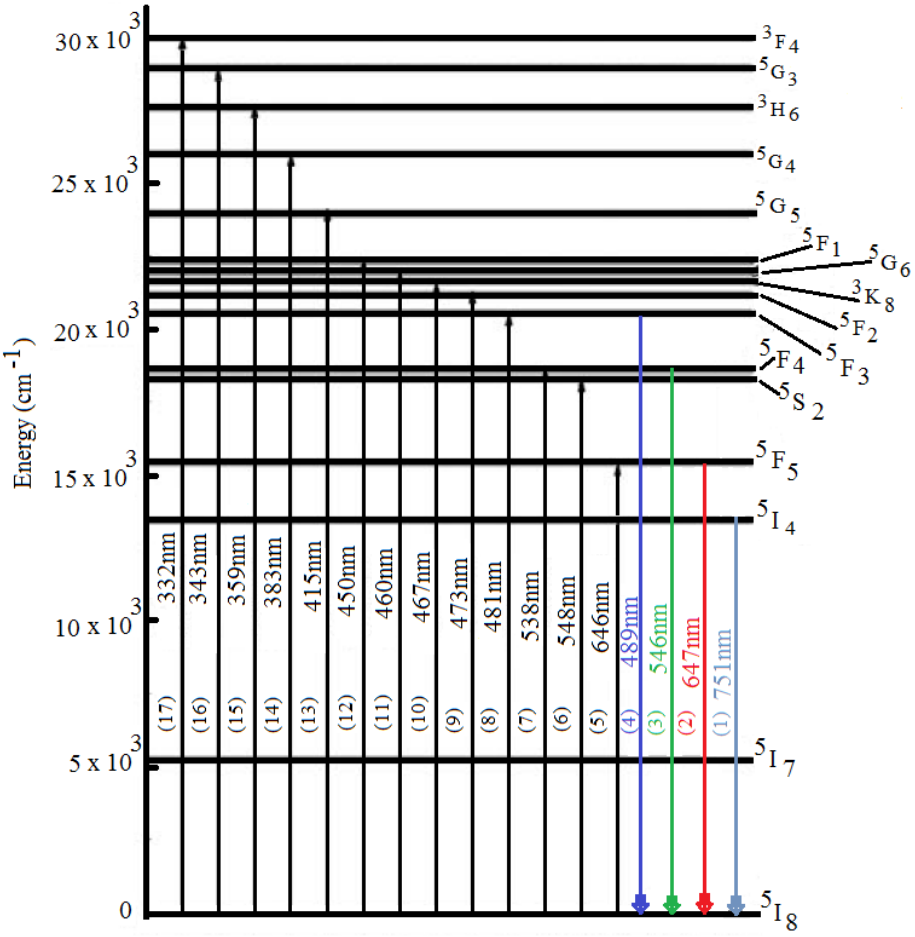
Energy (cm -1)
30 x 10 3
25 x 10 3
20 x 10 3
15 x 10 3
10 x 10 3
5 x 10 3
0
3F4
5G3
3H6
5G4
5G5
5F1
5G6
3K8
5F2
5F4
5F3
5S2
5F5
5I4
5I7
5I8
(17) 332nm
(16) 343nm
(15) 359nm
(14) 383nm
(13) 415nm
(12) 450nm
(11) 460nm
(10) 467nm
(9) 473nm
(8) 481nm
(7) 538nm
(6) 548nm
(5) 646nm
(4) 489nm
(3) 546nm
(2) 647nm
(1) 751nm

(b)

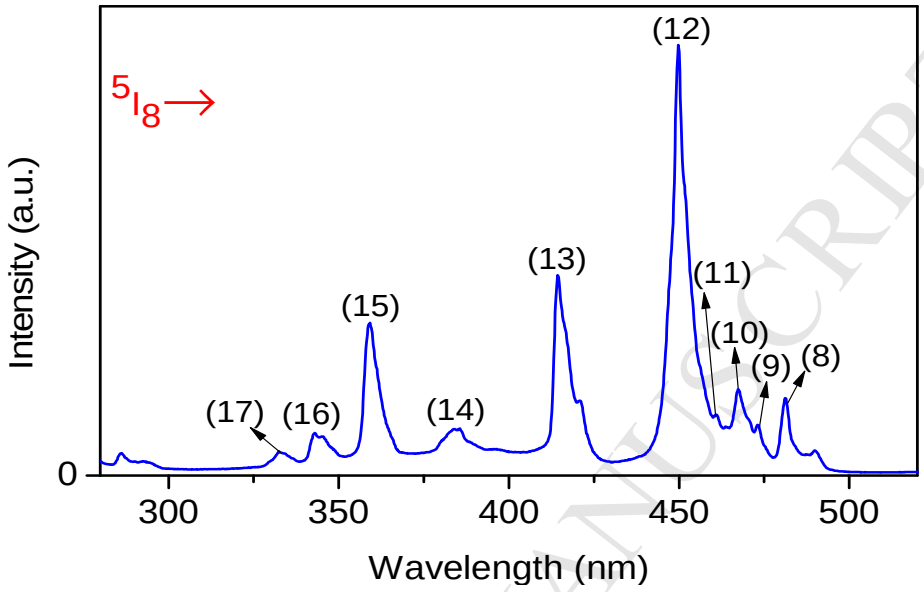

(c)

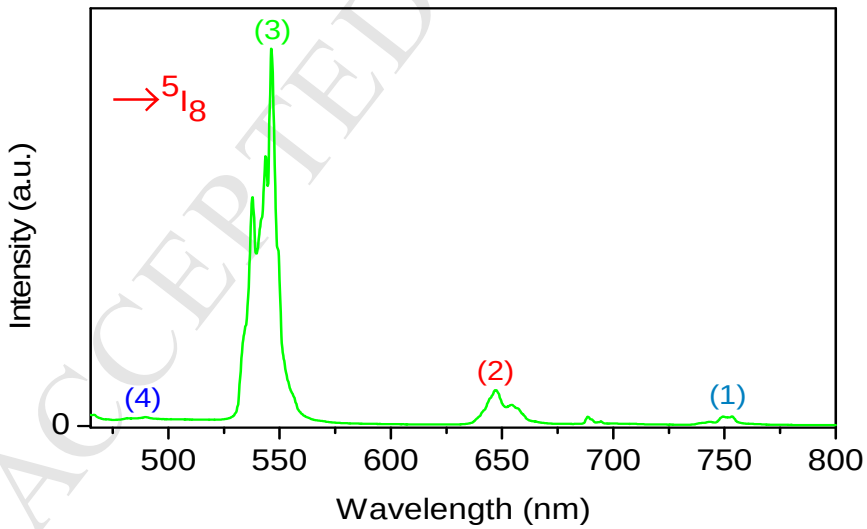

Fig. 3. (a) The transitions of the peaks are shown in energy level diagram of Ho^{3+} ion, (b) excitation spectrum of $CaAl_{12}O_{19}:Ho^{3+}$ phosphor (λ_{em}= 546 nm), and (c) Emission spectrum of $CaAl_{12}O_{19}:Ho^{3+}$ phosphor (λ_{ex}= 450 nm).

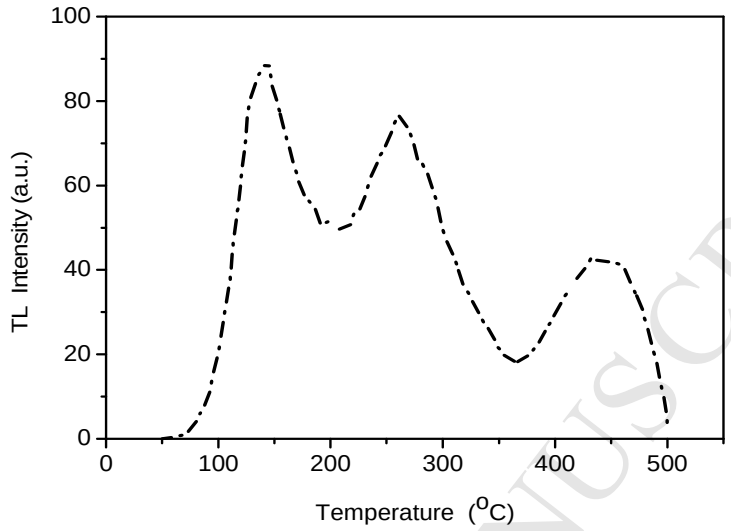

Fig. 4. TL glow curve of $CaAl_{12}O_{19}$:Ho at 4 °C/s for 50 Gy dose showing TL peaks at 140 °C, 260 °C and 440 °C respectively.

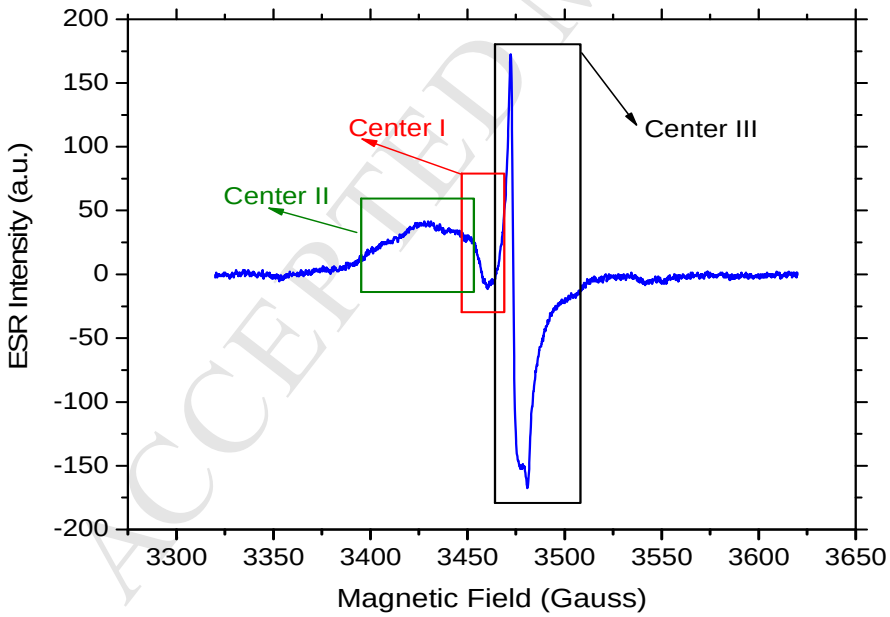

Fig. 5. (a) Room temperature ESR spectrum of irradiated $CaAl_{12}O_{19}$:Ho phosphor (gamma dose: 10 kGy). Line labelled as I is due to an O^- ion. Center II line is assigned to an O_2^- ion and center III is attributed to a F^+ center. (b) ESR spectrum at room temperature after warming the irradiated phosphor to 200 °C at a heating rate of 4 °C in the TL instrument.

(a)

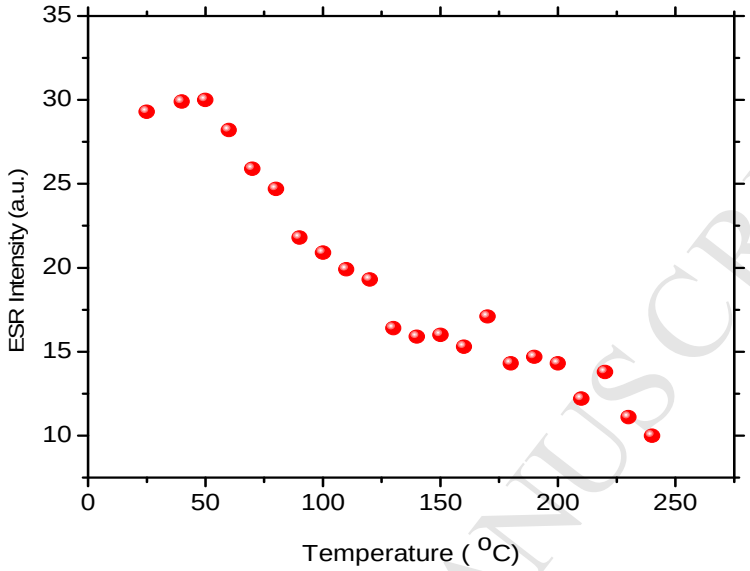

(b)

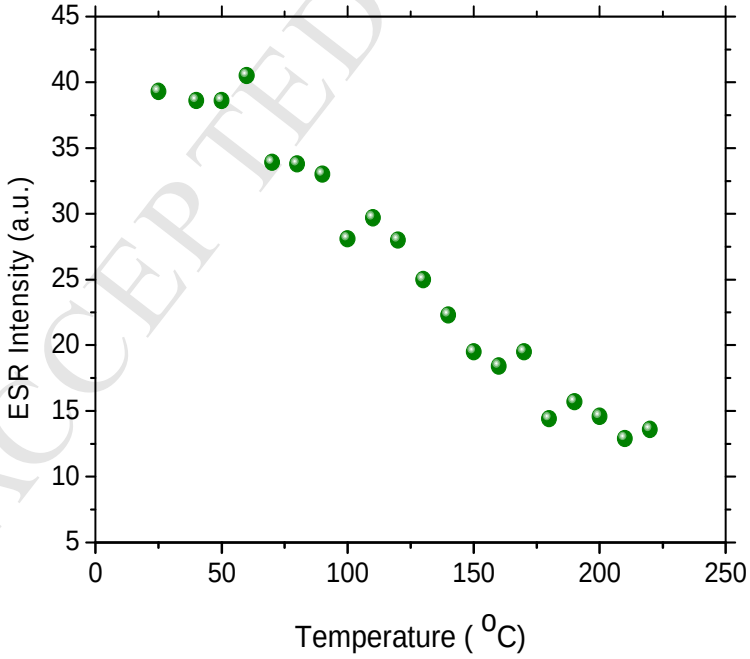

(c)

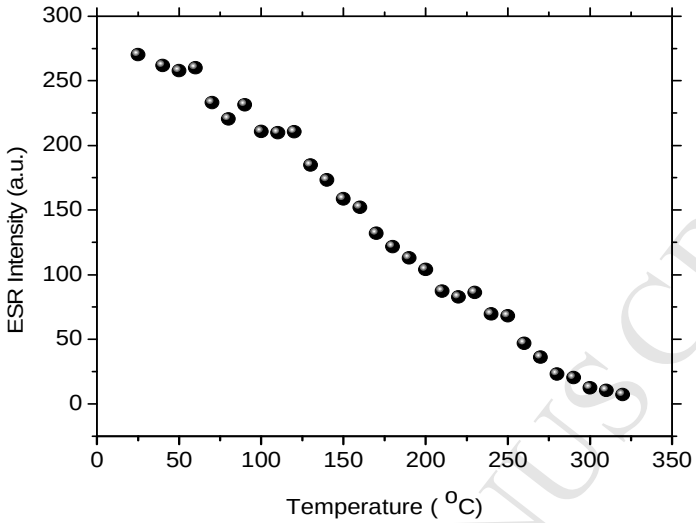

Fig. 6. Thermal annealing behaviour of (a) center I, (b) center II and (c) center III in $CaAl_{12}O_{19}$:Ho phosphor.

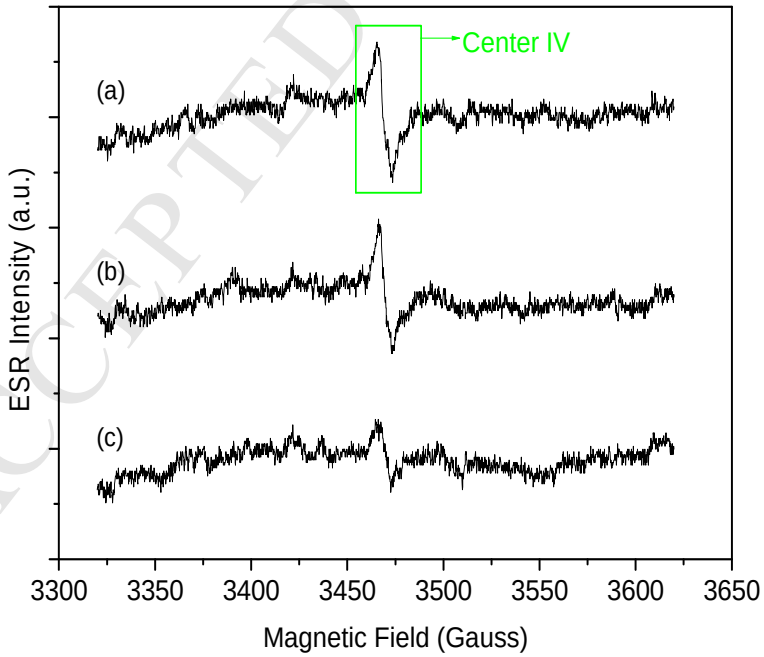

Fig. 7. Room temperature ESR spectrum of irradiated $CaAl_{12}O_{19}$:Ho phosphor after thermal anneal at (a) 300 °C, (b) 320 °C and (c) 500 °C showing center IV ESR line.

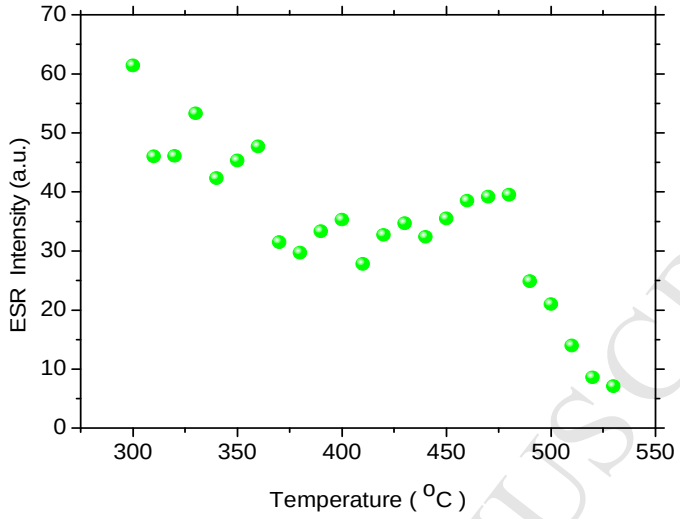

Fig. 8. Thermal annealing behaviour of center IV in $CaAl_{12}O_{19}$:Ho phosphor.

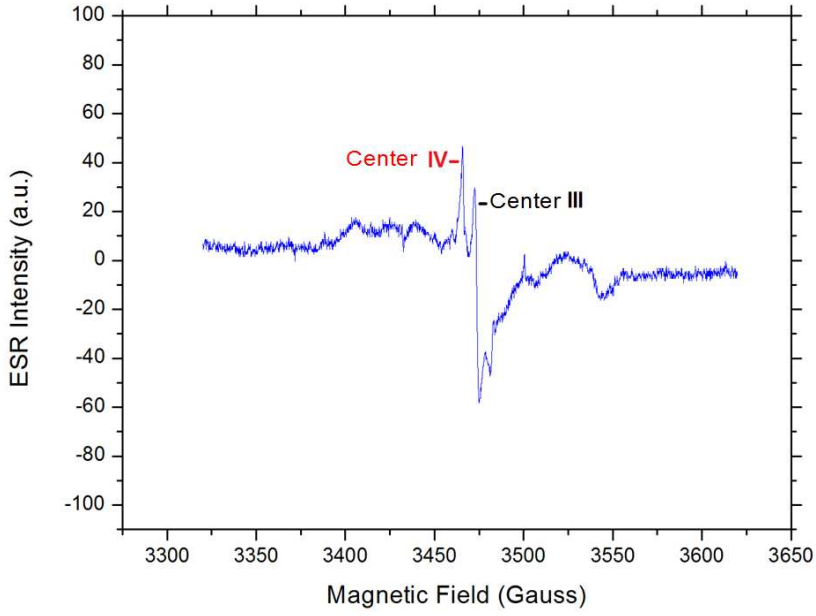

Fig. 9 Room temperature ESR spectrum of irradiated $CaAl_{12}O_{19}$:Ho phosphor (gamma dose: 10 kGy) after warming to 200 ^{o}C at a heating rate of 4 ^{o}C/S in the TL instrument

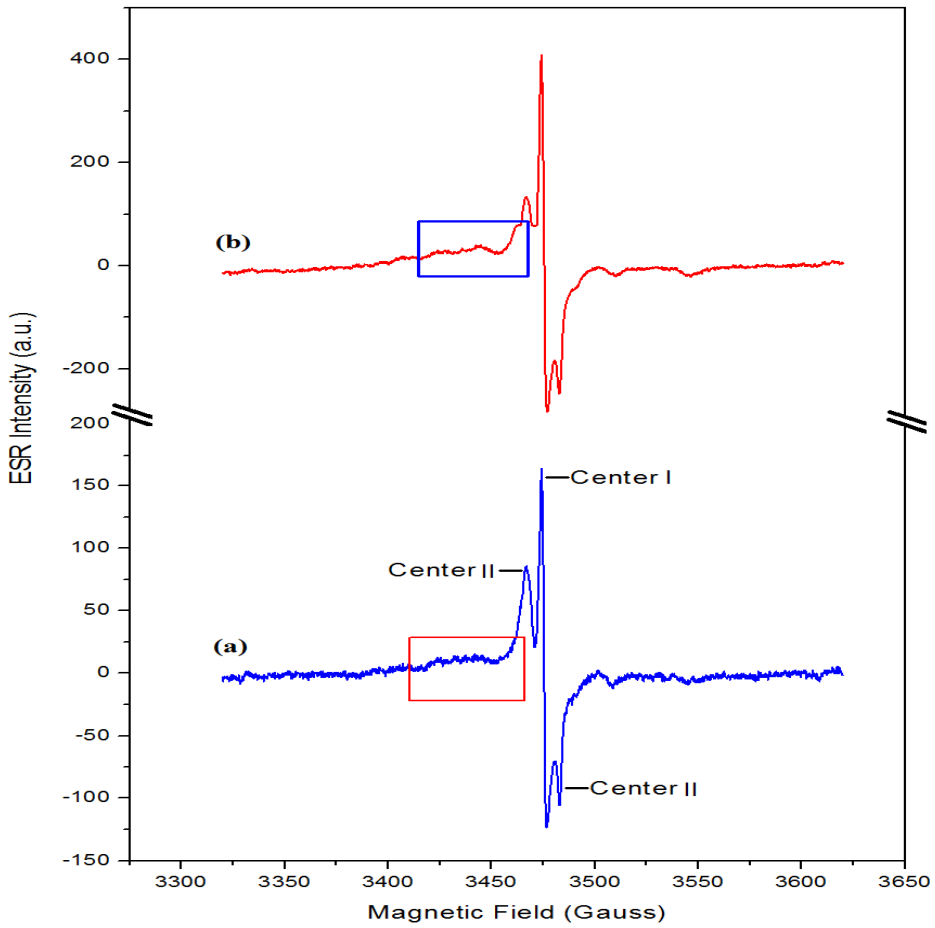

Fig. 10 (a) Room temperature ESR spectrum of irradiated pure $CaAl_{12}O_{19}$ (microwave power: 10 mW and 1 gauss modulation). (b) Spectrum recorded with higher microwave power and modulation (microwave power: 20 mW and 2 gauss modulation). The rectangular boxes show the lines arising from low intensity O^- and O_2^- ions.

► By facile combustion synthesis, Ho^{3+} doped $CaAl_{12}O_{19}$ powder phosphors obtained.

► Prepared phosphor was well characterized using XRD, PL, TL and ESR spectroscopy.

►Upon 450 nm light excitation, intense green emission observed.

► Defect centres were identified in gamma irradiated phosphor.